feature of this system is entirely consistent with purification below the eutectic; homogeneous nucleation of *p*-CNB in the drops will be inhibited by their decreasing size, and continued transfer of *m*-CNB from drops to crystals will take the liquid phase through the eutectic into the *p*-CNB side of the phase diagram.

To test this mechanism, emulsions having a *m*/*p* composition 90:10 were crystallized at temperatures of 30, 28, 24 and 22 °C and the emulsion droplet composition measured as a function of time (Fig. 3). At 24 and 22 °C the liquid phase does not have the eutectic composition (62.9%), but rather a composition richer in *p*-CNB, with respective crystal purities (Table 1) of 98.2 and 93.6% *m*-CNB.

Finally we took an emulsion of composition 60.9% *m*-CNB and crystallized it (with *m*-CNB seeds) at 15 °C, where we would expect a mixture of pure *p*-CNB and eutectic to crystallize. Contrary to this expectation, we obtained a final crystal purity of 65.5% *m*-CNB and a final liquid phase composition of 55.3% *m*-CNB. Thus enrichment of *m*-CNB was achieved on the *p*-CNB side of the eutectic, confirming that bypassing the eutectic is a real possibility in this emulsion system.

It is our belief that including a specific crystallization inhibitor for the unwanted component of the mixture (*p*-CNB here) would offer further enhancement of the separation by stabilizing the emulsion against crystallization at still lower temperatures. □

Received 20 February; accepted 23 May 1995.

1. Sloan, G. J. & McGhie, A. R. *Techniques of Chemistry* Vol. 18 (eds Weissberger, A. & Saunders, W.) (Wiley, New York, 1988).
2. Mullin, J. W. *Crystallisation* 309–323 (Butterworth Heinemann, London, 1993).
3. Fischer, O., Jancic, S. J. & Saxer, K. *Industrial Crystallisation* 84 (eds Jancic, S. J. & de Jong, E. J.) 153–157 (Elsevier, Amsterdam, 1984).
4. Cordiez, J. P., Grange, G. & Mutaftshchiev, B. *J. Colloid Interface Sci.* **85,** 431–441 (1982).
5. Turnbull, D. & Cech, R. E. *J. appl. Phys.* **21,** 804–810 (1950).
6. Skoda, W. & Van den Tempel, M. *J. Colloid Sci.* **18,** 568–584 (1963).
7. Chen, B. D., Garside, J., Davey, R. J., Maginn, S. J. & Matsuoka, M. *J. phys. Chem.* **98,** 3215–3221 (1994).
8. Garside, J. & Davey, R. J. *Chem. Engng Commun.* **4,** 393–424 (1980).

ACKNOWLEDGEMENTS. This work was supported by ZENECA p.l.c. from their Strategic Research Fund.

Interannual extremes in the rate of rise of atmospheric carbon dioxide since 1980

C. D. Keeling*, T. P. Whorf*, M. Wahlen* & J. van der Plicht†

* Scripps Institution of Oceanography, La Jolla, California 92093-0220, USA
† Center for Isotopic Research, University of Groningen, 9747 AG Groningen, The Netherlands

OBSERVATIONS of atmospheric CO_2 concentrations at Mauna Loa, Hawaii, and at the South Pole over the past four decades show an approximate proportionality between the rising atmospheric concentrations and industrial CO_2 emissions[1]. This proportionality, which is most apparent during the first 20 years of the records, was disturbed in the 1980s by a disproportionately high rate of rise of atmospheric CO_2, followed after 1988 by a pronounced slowing down of the growth rate. To probe the causes of these changes, we examine here the changes expected from the variations in the rates of industrial CO_2 emissions over this time[2], and also from influences of climate such as El Niño events. We use the $^{13}C/^{12}C$ ratio of atmospheric CO_2 to distinguish the effects of interannual variations in biospheric and oceanic sources and sinks of carbon. We propose that the recent disproportionate rise and fall in CO_2 growth rate were caused mainly by interannual variations in global air temperature (which altered both the terrestrial biospheric and the oceanic carbon sinks), and possibly also by precipitation. We suggest that the anomalous climate-induced rise in CO_2 was partially masked by a slowing down in the growth rate of fossil-fuel combustion, and that the latter then exaggerated the subsequent climate-induced fall.

An unexpected slowing in the rate of rise of atmospheric CO_2 appeared recently in measurements of CO_2 made at Mauna Loa Observatory, Hawaii and the South Pole (Fig. 1*a*). To study this and other interannual changes, both short-term and decadal, we have seasonally adjusted both records and then averaged them (Fig. 1*b*). The solid curve in the same panel depicts cumulative industrial emissions of CO_2 (mainly from the combustion of fossil fuels[2]) and shows the near proportionality of these emissions with the observed atmospheric CO_2 concentration increase. The fraction of cumulative emissions has been set to agree with the observed increase in atmospheric CO_2 between 1959 and 1979, a 20-year baseline period when industrial emissions grew at a nearly constant rate of 4.0% per year, leading to the expectation that a nearly constant fraction of these emissions should remain airborne (see p. 89 of ref. 3). By subtracting this curve of industrial emissions from the CO_2 record in Fig. 1*b*, disproportionate variations become clearly discernable (Fig. 1*c*).

To investigate the causes of these disproportionate variations, we first consider the expected influence of changes in the growth rate of industrial CO_2 emissions. To compute this influence, we have used a carbon-cycle model[1] which predicts the expected direct responses of the global terrestrial-biospheric and oceanic carbon reservoirs to industrial CO_2 emissions. The model accounts for changes in reservoir response directly related to the build-up of atmospheric CO_2, but not for the influence of environmental factors related to climatic variability.

With the model adjusted so that the observed fraction of industrial emissions over the 20-year baseline period remains airborne (55.9%), and provided that observed short-term fluctuations are disregarded, the predicted anomaly (Fig. 1*c*, dashed curve) fulfils the expectation of a constant airborne-fraction during the baseline period by having remained near zero, as did the observed anomaly. After 1980, however, the predicted anomaly fell steadily in response to an abrupt decrease in the growth rate of industrial emissions to an average of 1.7% (discernible in Fig. 1*b* as a decrease in upward curvature of the industrial trend after 1979). Changes after 1980 in the reported annual growth rate of industrial emissions[2] (data available to the end of 1991; 1% growth rate assumed for 1992 and 1993) are seen in Fig. 1*c* to have had little effect on the steadiness of the predicted downward trend. At the same time, the observed anomaly tends to rise, and, in spite of a steep decline after 1991, has remained above the model-predicted anomaly ever since.

The marked discrepancy between the predicted and observed anomalies on the decadal timescale after 1980, and differences throughout the record on shorter timescales, may be related to climate forcing involving air temperature[1], because anomalous variations in CO_2 and in temperature have tended to occur coherently, as suggested by comparing Fig. 2*a* with Fig. 2*b*. Many of these coherent anomalies are associated with El Niño events (arrows in Fig. 2*a*), but they also occur on the decadal timescale (solid curves) as previously noted by Keeling *et al.* (see p. 211 of ref. 1), and confirmed by a rigorous analysis of coherence[4]. On the decadal timescale a negative correlation of CO_2 with globally averaged precipitation over land is also suggested (Fig. 2*c*, note inverted plot).

Fluctuations in CO_2 associated with El Niño events have lagged those in temperature, as expected (see p. 211 of ref. 1) if the rate of change in CO_2 concentration were directly influenced by the temperature. In contrast, the decadal variations in temperature, and possibly in precipitation, almost directly correlate with the CO_2 concentration itself. If these decadal correlations are significant, it seems evident that the onset of a climate change, such as a warming trend, has a measurable influence on the atmospheric CO_2 concentration, but that if the climate change is sustained, its further influence gradually weakens. Possible reasons for this weakening influence may involve time delays between coupled processes of uptake and release of carbon, for example between perturbations in photosynthesis and respiration of plant communities.

To add further to our understanding of the possible causes of these anomalous changes in CO_2, we have compared variations in the concentration of atmospheric CO_2 with variations in the $^{13}C/^{12}C$ isotopic ratio of this gas in air collected at both Mauna Loa Observatory and the South Pole (Fig. 3*a* and *b*). By taking into account isotopic fractionation of carbon in the major pathways of the global carbon cycle, we have attempted to distinguish the contributions to the atmospheric CO_2 anomaly caused separately by gas exchanges with the terrestrial biosphere and with the oceans[1,5]. This calculation, which has been called a "double deconvolution[1]", is not without uncertainty, because the isotopic fractionation factors and ratios involved in the pathways and reservoirs of the carbon cycle are not accurately known, and the signal associated with El Niño events is relatively

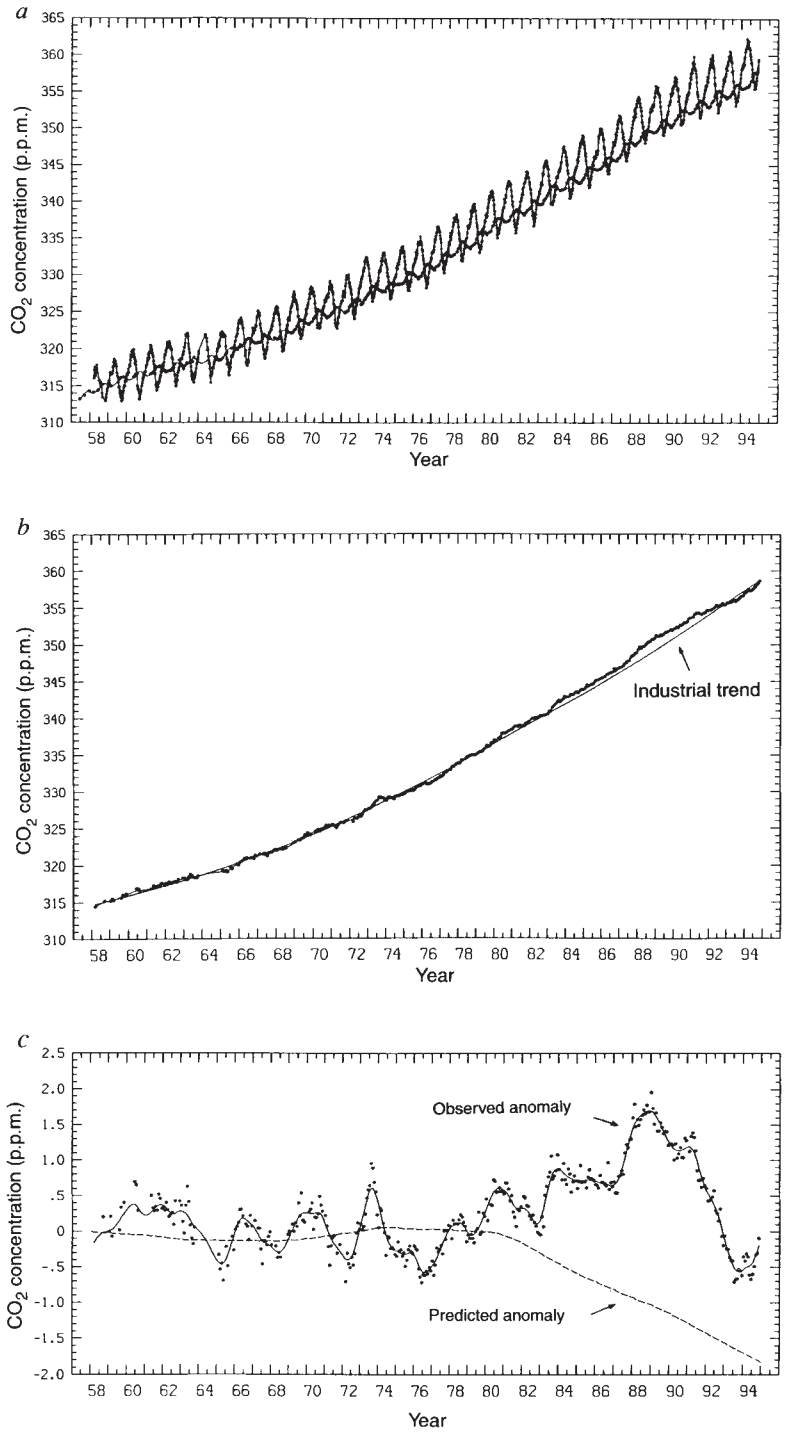

FIG 1 Time trend in the concentration of atmospheric CO_2, in parts per million by volume (p.p.m.), compared to emissions of CO_2 from fossil-fuel combustion. *a*, The concentrations of CO_2 at Mauna Loa Observatory, Hawaii (20° N, 156° W) and at the South Pole through November 1994. The former record is distinguished by its pronounced seasonal cycle. For Mauna Loa, weekly data are shown as dots and connected with straight lines. For the South Pole, monthly data points are shown as dots, and connected approximately by a smooth curve (see p. 167 of ref. 1). *b*, The average of the above records (dots connected by a smooth curve as in *a* for the South Pole) after seasonal adjustment of monthly averages at both stations, compared to a curve (solid line, labelled 'industrial trend') of a fixed fraction (55.9%) of the cumulative industrial emissions of CO_2 from fossil fuel combustion and cement production[2]. This fraction was chosen to bring exact agreement between the observations and cumulative industrial emissions between 1 January 1959 and 1 January 1979, and is almost the same fraction as realized over the entire record. *c*, Observed CO_2 anomaly obtained by subtracting the industrial emissions curve in *b* from the monthly CO_2 data. The solid curve is a spline fit[1,17] to the monthly data with a standard error, σ, of 0.096 p.p.m., selected to emphasize the fluctuating character of the record on the timescale of El Niño events (large-scale, coherent climate anomalies associated with a collapse of the trade winds over the Pacific ocean[18,19]). The dashed curve depicts a predicted CO_2 anomaly, in which it is assumed that variability in atmospheric CO_2 is caused solely by industrial CO_2 emissions modified by the direct responses of the global terrestrial biospheric and the oceanic carbon reservoirs to these emissions, neglecting any effect of climate factors. The prediction is based on a carbon-cycle model[1], in which the oceanic carbon reservoir is assumed to transport carbon by vertical diffusion at a rate that reproduces the observed uptake of radiocarbon, and the terrestrial biosphere is assumed to respond to higher CO_2 concentrations by more rapid plant growth. A global growth factor was set to 0.114 so that a constant fraction (55.9%) of industrial CO_2 emissions is predicted to remain in the atmosphere between 1959 and 1979.

weak. Nevertheless, the results of double deconvolution suggest an explanation for the observed anomalies in CO_2 concentration which we believe to be qualitatively correct.

As shown in Fig. 3*c* and *d*, the inferred separate biospheric and oceanic fluxes contributing to the CO_2 anomaly, since 1978 when our isotopic record began, have tended to oppose each other, with increases in biospheric sources and anomalous oceanic sinks occurring at times of rising CO_2 anomaly (Fig. 2*a*) and the reverse occurring at times of falling CO_2 anomaly[1]. The period of sharply falling anomaly after mid-year 1991 is an exception, in which for slightly over a year, sinks are indicated for both fluxes[6], perhaps a rare event in light of our analysis of El Niño events.

Disregarding short-term interannual fluctuations, the anomalous oceanic flux, in the 12.5 years of isotopic record before June 1991, was a source of 3.0 Gt C, consistent with significant warming of surface water which occurred during this period (see p. 204 of ref. 1). The overall negative biospheric flux of 1.2 Gt C, for the same period only partially offsets this oceanic source. In contrast, for approximately the next two years (June 1991 to September 1993) the anomalous oceanic flux was negligible while the biospheric flux represented a strong sink of 3.0 Gt C.

Taking note of the short-term fluctuations in global CO_2 anomaly plotted in Fig. 2*a*, one sees successively higher minima in 1979, 1982, 1986 and 1990 in advance of El Niño events. After the minimum in 1990, the rise was brief, however, being cut short in mid-year 1991 by a steep decline. Is the Pinatubo volcanic eruption[7] of June 1991 implicated in this dramatic downward anomaly? A search for a connection between this event and the carbon cycle is complicated by weak El Niño conditions which were present during both 1992 and 1993 in the tropical Pacific[8]. Our double-deconvolution calculation suggests that the oceans typically are a larger sink for atmospheric CO_2 during El Niño events than otherwise[1,9], whereas the terrestrial biosphere is the reverse. The inferred anomalous oceanic sink of 0.6 Gt C immediately after the Pinatubo eruption (Fig. 3*d*), although weak and soon cancelled by a weak source in 1993, is consistent with this explanation. The biosphere, however, unlike other recent El Niño events, was also a sink as noted above.

Cooling produced by volcanic aerosols from the eruption might explain this unusual biospheric sink, especially if the sink preceding it in 1989 and 1990 was mainly a recovery from a biospheric source during the El Niño event that began in 1987. The magnitude of the post-1991 cooling trend, shown in Fig. 2*b*, although less precipitous than the fall in the CO_2 anomaly, was greatest during the northern summer months (see short-dashed portion of curve in Fig. 2*b*). This cooling, if it was accompanied by increased precipitation at appropriate locations in the Northern Hemisphere, may have appreciably enhanced plant growth (see p. 167 of ref. 10) or reduced the release of CO_2 by soil respiration and wildfires.

Perhaps, however, the Pinatubo eruption was only incidental to a declining CO_2 anomaly. The unusually warm temperatures preceding the eruption may have caused an increase in photosynthesis and hence in net biospheric uptake of CO_2 over the whole period of falling CO_2 anomaly after 1988. A substantial

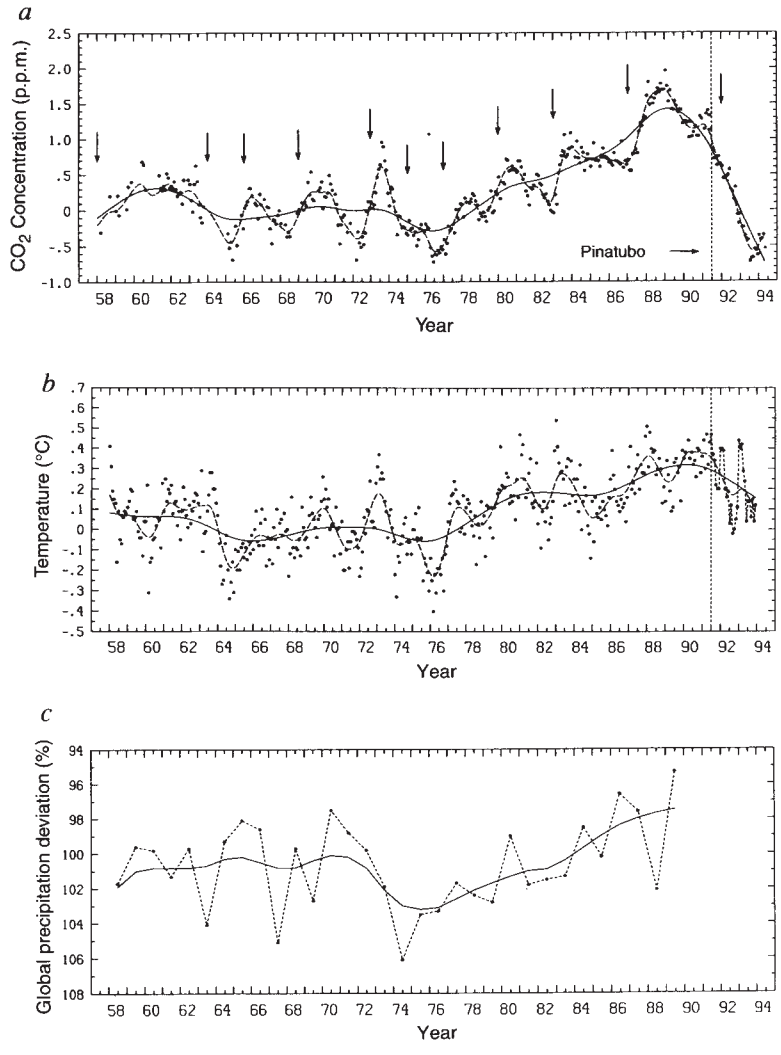

FIG 2 Comparison of the interannual variability of anomalies in atmospheric CO_2, surface air temperature and atmospheric precipitation. *a*, Monthly CO_2 anomalies as shown previously in Fig. 1c except that the previously solid curve is now shown as a dashed curve, and the data extend only through May 1994. The new solid curve represents a spline fit (σ = 0.129 p.p.m.) to emphasize decadal timescale variability. Vertical arrows indicate times of El Niño events[1,8,20]. A vertical line, also shown in *b*, indicates the time of the main eruption of Mt Pinatubo[7]. *b*, A similar plot of global land and oceanic near-surface air temperature variability (σ is 0.121 and 0.230 °C for dashed and solid curves, respectively). The monthly data, to and including 1993, are from refs 21–24 and P. D. Jones, personal communication). c, Plot of percentage deviations from the mean in global precipitation over land to 1989, reproduced from Fig. 17 of Eischeid *et al.*[25] inverted to emphasize a negative correlation of precipitation with CO_2 on the decadal timescale. The dashed line connects annual averages shown as dots. The solid line, from the original figure, is a smoothed representation to indicate long-timescale variations.

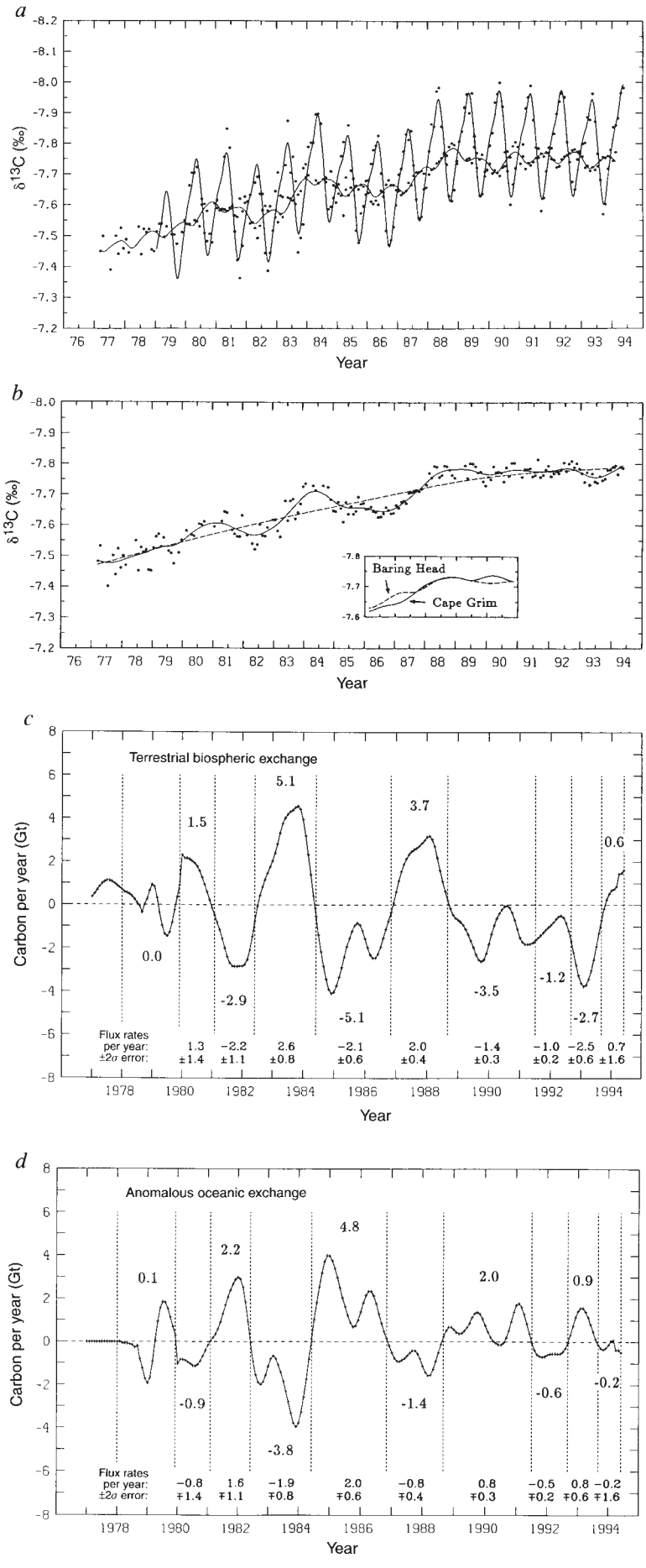

FIG 3 Time trend in the reduced isotopic ratio, $\delta^{13}C$, of atmospheric CO_2 from 1977 through early 1994, shown together with time plots of interannual exchanges of atmospheric CO_2 by the oceans and terrestrial biosphere. The exchanges are inferred from these isotopic data in combination with the atmospheric CO_2 data shown in Fig. 1*a*. *a*, The reduced isotopic ratio, $\delta^{13}C$ at Mauna Loa Observatory and the South Pole, the former record distinguished by its pronounced seasonal cycle (compare Fig. 1*a*). The ratio $\delta^{13}C$ is defined as $(R/R_0)-1$, where R denotes the $^{13}C/^{12}C$ ratio of the sampled gas and R_0 is the corresponding ratio of the international carbonate standard, PDB. The data, in per mil (‰), are shown as monthly averages by dots and the trends by solid curves (compare Fig. 1*a*). *b*, The average of the above records after seasonal adjustment (compare Fig. 1*b*). The data have a standard error, σ, of 0.024 (‰) relative to the solid curve, which follows the interannual trend as closely as possible, and a σ of 0.037 (‰) relative to the stiffer dashed curve, in which shorter-term interannual variations are suppressed by decreasing the squared second derivative of the fitting function[26]. Inset, similar trends at Baring Head, New Zealand (41° S, 175° E) from data measured in our laboratory (dashed line) and at Cape Grim, Tasmania (41° S, 145° E) as reported by Francey *et al.*[16] (solid line). These trends show a lesser-amplitude El Niño signal, as discussed in the text. The σ values of these curves (0.042 and 0.029 ‰, respectively) were set using data from 1985 to 1991 to give the same squared second derivative[26], so that the stiffnesses are the same. *c*, Time trend in the exchange of CO_2 by the terrestrial biosphere with the atmosphere, determined by a double deconvolution and shown as a solid curve, in Gt C yr^{-1} (where Gt C denotes 10^{12} kg of carbon). The calculation of CO_2 solubility in sea water assumes constant temperature (also in Fig. 3*d*). The exchanges are not adjusted to sum to zero over the full record (as in ref. 1, Figs 55 and 56) and thus their averages over the full record reflect the oceanic vertical diffusion rate assumed in the double deconvolution[1]. Vertical lines separate periods of persistent positive and negative fluxes whose intergrated fluxes are shown numerically in Gt C, directly above or below the curve. They are defined by the zero crossings in *d*. Flux rates are shown at the bottom of the panel in Gt C yr^{-1} with estimates of their statistical error expressed as 2σ (95% confidence level). *d*, Residual (anomalous) exchange of CO_2 by the oceans, determined by the double deconvolution after allowing for oceanic absorption of CO_2 predicted in response to industrial CO_2 emissions and the isotopic disequilibrium attending that response. The periods of integration, shown by vertical lines, define alternations between positive and negative fluxes that approximate warm and cold phases of El Niño events. The statistical error analysis was performed by carrying out a second double deconvolution, assuming the stiffer dashed curve of Fig. 3*b* in place of the solid curve. The difference in Gt C over each interval of integration, found by comparing the two double deconvolutions, was taken as the basis for scaling the statistical error in flux to the error in the trend in $\delta^{13}C$, the latter being approximated by a straight-line fit to the data of the interval. Because the flux is proportional to the slope, the error in flux is proportional to the error in the slope. Computed errors in $\delta^{13}C$ contribute equally and oppositely to the biospheric and oceanic fluxes, because these sum to the flux obtained by the better-constrained single deconvolution calculation (see p. 202, equation 6.6 of ref. 1) based only on concentration data which we assume to contribute no error. This statistical analysis does not address unidentified systematic biases in the data.

increase in the amplitude of the seasonal oscillation of atmospheric CO_2 from 1989 through 1993 (we calculate an 8% increase at Mauna Loa, Hawaii, compare Fig. 1*a*) suggests this possibility. Or perhaps cooling related to the Pinatubo eruption and antecedent warming both contributed to a biospheric sink after 1989.

Changes in human land use, especially deforestation, have added further emissions of CO_2 to the air in recent years, and may partially account for the rising CO_2 anomaly after 1979. This is difficult to prove, however, because little information exists to establish annual rates of CO_2 emissions from land-use change[11]. Even the global average emission rate since 1979 is poorly known, as indicated by a wide range of estimates[12] (0.4–2.6 Gt C yr^{-1}). It is not likely, however, that a substantial part of the shift from an upward to a downward-tending anomaly after 1988 was due to land-use changes. The decrease in CO_2 emission rate required to explain the shift is too large, being approximately 1.4 Gt C yr^{-1} after taking into account that oceanic CO_2 exchange must partially offset biospheric exchange, as it does with respect to industrial emissions. Some decrease in deforestation may have occurred about this time[13,14], but almost surely not a decrease approaching 1.4 Gt C yr^{-1}, a change greater than half of the upper limit of the global emission rate from land-use change, quoted above. Therefore, the shift is more likely to reflect mainly natural causes, most evident in the correlation of CO_2 anomalies with temperature, seen in Fig. 2*a* and *b*.

In summary, the slowing down of the rate of rise of atmospheric CO_2 from 1989 to 1993, seen in our data and confirmed by other measurements[6,15], is partially explained (about 30% according to Fig. 1*c*) by the reduction in growth rate of industrial CO_2 emissions that occurred after 1979. We further propose that warming of surface water in advance of this slowdown caused an anomalous rise in atmospheric CO_2, accentuating the subsequent slowdown, while the terrestrial biosphere, perhaps by sequestering carbon in a delayed response to the same warming, caused most of the slowdown itself.

In contradiction to some of our findings, Francey *et al.*[16] have recently suggested that isotopic data for atmospheric CO_2 from Cape Grim, Tasmania (41° S) and elsewhere do not show an El Niño signal. For the 1983 El Niño event their data in this respect clearly disagree with our data at Mauna Loa and the South Pole[1], but the comparison is not rigorous because we lack data for the vicinity of Cape Grim. For the 1987 event, however, we have data for Baring Head, New Zealand, a station at nearly the same latitude as Cape Grim, and they have data for the South Pole[16]. Our New Zealand data show an El Niño signal that is a little more than half as strong as we find for the South Pole and Mauna Loa averaged. This weaker signal agrees well with a signal which we find in their Cape Grim data after seasonal adjustment (Fig. 3*b* inset), a signal which, however, was reduced in their analysis by smoothing (their Fig. 1*a*).

Furthermore, their data for the South Pole show a signal similar to ours for the 1987 event, although they did not include these data in the computation of sources and sinks of CO_2. On the basis of the near agreement of our and their data sets at both latitudes, it seems plausible that El Niño isotopic signals are generally weaker in the middle of the Southern Hemisphere than elsewhere, perhaps a consequence of isotopic air–sea exchange. (We find no corresponding diminution in the concentration signal in the middle of the Southern Hemisphere.) Thus, Francey *et al.* may have reached a conclusion contrary to ours by focusing on their isotopic data for a single station (Cape Grim) where the El Niño signal may be weaker. Thus, we believe that our isotopic data are correct in inferring opposing global oceanic and terrestrial El Niño CO_2 signals, although these may have been exaggerated by our not taking into account isotopic data in the middle of the Southern Hemisphere.

We point out, in closing, that the unprecedented steep decline in the atmospheric CO_2 anomaly ended late in 1993 (see Fig. 1*c*). Neither the onset nor the termination was predictable. Environmental factors appear to have imposed larger changes on the rate of rise of atmospheric CO_2 than did changes in fossil fuel combustion rates, suggesting uncertainty in projecting future increases in atmospheric CO_2 solely on the basis of anticipated rates of industrial activity. □

Received 17 May; accepted 27 April 1995.

1. Keeling, C. D. *et al. Aspects of Climate Variability in the Pacific and the Western Americas* (ed. Peterson, D. H.) 165–236 (Geophys. Monogr. 55, Am. Geophys. Union, Washington DC, 1989).
2. Andres, R. J., Marland, G., Boden, T. & Bischof, S. in *Proc. of the 1993 Global Change Inst. on the Carbon Cycle* (eds Wigley, T. & Schimel, D.) (Cambridge Univ., London, in the press).
3. Bacastow, R. B. & Keeling, C. D. in *Workshop on the Global Effects of Carbon Dioxide from Fossil Fuels*, CONF-770385 (eds Elliot, W. P. & Machta, L.) 72–90 (US Dept. of Energy, Washington DC, 1979).
4. Kuo, C., Lindberg, C. & Thomson, D. J. *Nature* **343,** 709–714 (1990).
5. Heimann, M. & Keeling, C. D. in *Aspects of Climate Variability in the Pacific and the Western Americas* (ed. Peterson, D. H.) 237–275 (Geophys. Monogr. 55, Am. Geophys. Union, Washington DC, 1989).
6. Whorf, T. P., Keeling, C. D. & Wahlen, M. *Climate Modeling & Diag. Lab.* Vol. 21, 119–122 (Summary Report 1992, NOAA, Boulder, CO, 1993).
7. Hansen, J., Lacis, A., Ruedy, R. & Sato, M. *Geophys. Res. Lett.* **19,** 215–218 (1992).
8. Halpert, M. S. *et al. Eos* **74,** 433–439 (1993).
9. Winguth, A. M. E. *et al. Globl biogeochem. Cycles* **8,** 39–63 (1994).
10. Larcher, W. *Ökologie der Pflanzen* (Eugen Ulmer, Stuttgart, 1984).
11. Houghton, R. A. *Bioscience* **44,** 305–313 (1994).
12. Dale, V. H., Houghton, R. A. & Hall, C. A. S. *Can. J. For. Res.* **21,** 87–90 (1991).
13. Fearnside, P. M. *Ambio* **22,** 537–545 (1993).
14. Grubb, M. *Nature* **368,** 489 (1994).
15. Conway, T. J. *et al. J. geophys. Res.* **99,** 22831–22855 (1994).
16. Francey, R. J. *et al. Nature* **373,** 326–330 (1995).
17. Sarmiento, J. L. *Nature* **365,** 697–698 (1993).
18. Rasmusson, E. M. & Wallace, J. M. *Science* **222,** 1195–1202 (1983).
19. Wyrtki, K. *J. geophys. Res.* **90,** 7129–7132 (1985).
20. Rasmusson, E. M. *Oceanus* **27,** 5–12 (1984).
21. Jones, P. D. *et al. J. Clim. appl. Met.* **25,** 161–179 (1986).
22. Jones, P. D., Raper, S. C. B. & Wigley, T. M. L. *J. Clim. appl. Met.* **25,** 1213–1230 (1986).
23. Jones, P. D., Wigley, T. M. L. & Wright, P. B. Report No. NDP-022/R1, CDIAC (Oak Ridge Nat. Lab., 1990).
24. Jones, P. D. & Briffa, K. R. *Holocene* **2,** 165–179 (1992).
25. Eischeid, J. K. *et al.* Tech. Rep. TR051 (US Dept. of Energy, Washington DC, 1991).
26. Bacastow, R. B., Keeling, C. D. & Whorf, T. P. *J. geophys. Res.* **90,** 10529–10540 (1985).

ACKNOWLEDGEMENTS. We thank P. Jones for providing monthly global average surface air temperature data. We also thank H. Diaz, M. Heimann, R. Bacastow, K. Egan, R. Keeling and S. Piper for their advice. This work was supported by the Division of Atmospheric Science of the USNSF the US Department of Energy and NASA.

Archaean subduction inferred from seismic images of a mantle suture in the Superior Province

A. J. Calvert*, E. W. Sawyer†, W. J. Davis‡§ & J. N. Ludden‖§

* Département de Génie Minéral, Ecole Polytechnique, CP 6079, succ. centre-ville, Montréal, Québec H3C 3A7, Canada
† Département des Sciences Appliquées, Université du Québec à Chicoutimi, Chicoutimi, Québec G7H 2B1, Canada
‡ GEOTOP, Université du Québec à Montréal, CP 6888, succ. centre-ville, Montréal, Québec H3C 3P8, Canada
‖ Département de Géologie, Université de Montréal, CP 6128, succ. centre-ville, Montréal, Québec H3C 3J7, Canada

PLATE tectonics provides the basis for the interpretation of most current terrestrial tectonic activity, and is widely accepted as having been active over much of the Earth's history[1]. Yet the timing of initiation of this process is subject to debate[2–9]. So far, the earliest seismic evidence for plate tectonics has come from a fossil mantle suture in the Svecofennian orogen (1.89 Gyr ago)[10] and

§ Present addresses: Geological Survey of Canada, 601 Booth Street, Ottawa, Ontario K1A 0E8, Canada (W.J.D.); Centre de Recherches Pétrographiques et Géochimiques, 15 Rue Notre Dame des Pauvres, 54401 Vandoeuvre-les-Nancy, BP 20 Cedex, France (J.N.L.).